Dispersion management with microstructured optical fibers: ultraflattened chromatic dispersion with low losses

G. Renversez and B. Kuhlmey

Institut Fresnel (Unité Mixte de Recherche 6133, Centre National de la Recherche Scientifique), Faculté des Sciences et Techniques de St. Jérôme, Avenue Escadrille Normandie-Niémen, 13397 Marseille Cedex 20, France

R. McPhedran

School of Physics, University of Sydney, Sydney, NSW 2006, Australia

Received January 7, 2003

We numerically demonstrate ultraflattened chromatic dispersion with low losses in microstructured optical fibers (MOFs). We propose using two different MOF structures to get this result. Both structures are based on a subset of a triangular array of cylindrical air holes; the cross sections of these inclusions are circular, and a missing hole in the fiber's middle forms the core. In this MOF structure the diameters of the inclusions increase with distance from the fiber axis until the diameters reach a maximum. With this new design and with three different hole diameters, it requires only seven rings to reach the 0.2-dB/km level at $\lambda = 1.55$ μm with a variation amplitude of dispersion below 3.0×10^{-2} ps nm^{-1} km^{-1} of $\lambda = 1.5-1.6$ μm. With the usual MOF (made from holes of identical diameter), we show that at least 18 hole rings are required for losses to decrease to <1 dB/km at $\lambda = 1.55$ μm. © 2003 Optical Society of America

OCIS codes: 060.2270, 060.2280, 060.2400, 060.2430.

Microstructured optical fibers (MOFs) were quite recently proposed as new tools for dispersion management in optical communication systems.[1] Several studies[2,3] in which a vector method with periodic boundary conditions was used[4] were made to design such MOFs; nevertheless, as was recently shown,[5] one must take the finite cross sections of MOFs into account to describe accurately the chromatic dispersion properties of such fibers and to compute the losses. Moreover, comparison of the computed dispersion curves and the experimental results remains difficult.[6]

A mode of a MOF is characterized by the mode's field pattern and its effective indices $n_{\text{eff}} = \beta/k_0$, where β is its propagation constant and $k_0 = 2\pi/\lambda$ is the free-space wave number. Because of the finite transverse extent of the confining structure, the effective index is a complex value; its imaginary part $\Im(n_{\text{eff}})$ is related to losses $\mathcal{L}$ (in decibels per meter) through the relation $\mathcal{L} = 40\pi\, \Im(n_{\text{eff}}) \times 10^6/[\lambda \ln(10)]$, where λ is given in micrometers. Dispersion parameter D is computed through the usual formula from the real part of effective index $\Re(n_{\text{eff}})$ (Ref. 7): $D = -(\lambda/c)\partial^2\, \Re(n_{\text{eff}})/\partial\lambda^2$. We have developed a multipole method[8] that allows us to compute accurately the complex effective index of the modes of a wide variety of MOFs. Our method has been verified by comparison with other numerical methods.[5,9,10]

In what follows, we simulate plain core MOFs made from a subset of a triangular array of cylindrical air inclusions ($n_i = 1$). The inclusion spacing, or pitch, is denoted Λ. The inclusions are circular, possibly with various diameters, and lie about a core that is in fact a missing central inclusion. The matrix and the jacket are made from silica, so the guiding structure is formed by a finite number N_r of rings of air holes in infinite bulk silica whose Sellmeier expansion (which does not include material losses) is taken from Ref. 7. Our aim in this study is to establish MOF designs that combine ultraflattened chromatic dispersion together with low losses near the telecommunication wavelength $\lambda = 1.55$ μm. We exhibit two designs that achieve this objective. The first contains air holes of one diameter and requires 18 rings of holes for losses smaller than 1 dB/km. The second utilizes air holes with three different diameters, which yield ultraflat dispersion and even lower loss levels with only seven rings.

Chromatic dispersion in MOFs arises from that of the silica (D_{mat}) and also from the waveguide dispersion (D_W) associated with the structure of the confining region. Note that our multipole method provides directly the total dispersion (D), so we deduce D_W from the relation $D_W \simeq D - D_{\text{mat}}$. As was pointed out by Ferrando *et al.*,[2] it is convenient to achieve a specific total dispersion by controlling D_W to make it follow a trajectory parallel to that of $-D_{\text{mat}}$ in the target wavelength interval. The parameters with which one can achieve this are hole diameter d, pitch Λ, and number of rings N_r.[5]

From a previous theoretical work,[11] we choose $d/\Lambda < 0.406$ to guarantee single-mode operation of the MOF design.

In Fig. 1 we show the variation of total dispersion D with the number of rings of six normal MOF geometries, all located in the region of stable dispersion. All curves show a simple variation with N_r, which can be modeled accurately by an exponential form $D_1 \exp(-\kappa N_r) + D_{\text{lim}}$. Such a fitting form has three parameters (D_1, κ, D_{lim}), which can be determined accurately from the results of $N_r = 3-6$. This procedure has important advantages because MOFs with relatively small numbers of rings are relatively quickly modeled; yet we have established that the exponential fit thereafter accurately describes the dispersion of much larger structures and even limiting parameter D_{lim}, the dispersion of a mode pinned by a single defect in an infinite lattice. In fact, using the limit dispersion D_{lim} determined numerically for a

0146-9592/03/120989-03$15.00/0

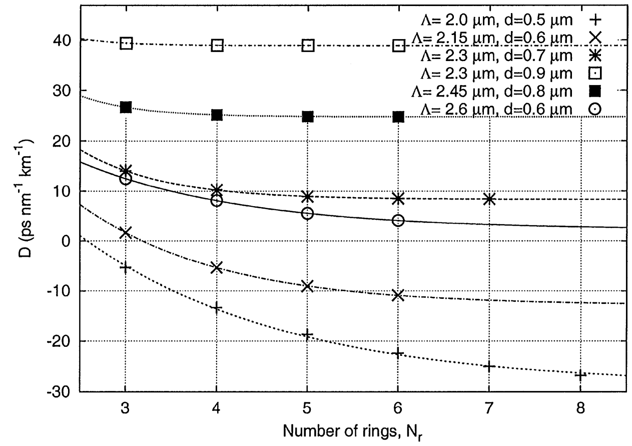

Fig. 1. Dispersion decay at $\lambda = 1.55\ \mu$m as a function of the total number of hole rings N_r for several MOF structures. Λ is the hole spacing, and d is the hole diameter. The points correspond to the computed numerical dispersion; the curves, to exponential based fits.

set of values of wavelength λ, we can also determine $S_{\mathrm{lim}} = \partial D_{\mathrm{lim}}/\partial\lambda$, the limit dispersion slope.

In Fig. 2 we show the variations of these important parameters D_{lim} and S_{lim} as a function of hole diameter d for several pitches Λ. This figure illustrates well how one can isolate a MOF that exhibits a target dispersion value for a sufficiently large number of rings N_r, which is flat over a range about the chosen wavelength value. Indeed, such a MOF will have the desired value of D_{lim} and simultaneously a value of S_{lim} close to zero. Note that the pitches exhibited in Fig. 2 were chosen carefully to exemplify this desirable behavior. We have also shown that, for the data of Fig. 2, the minima of S_{lim} as a function of d occur in the same diameter interval (0.65; 0.7 μm) for all MOFs that have $N_r \geq 6$. From Fig. 2, if one requires a positive nearly zero flat chromatic dispersion, then, using these curves, one should start the dispersion engineering with a MOF such that $\Lambda = 2.45\ \mu$m and $d = 0.6\ \mu$m. Of course, Fig. 2 can be used to isolate MOF geometries that have different characteristics, such as a prescribed slope with a fixed average value of dispersion over a wavelength range.

In Fig. 3 we show dispersion characteristics for three MOF designs. At the top, the total dispersion is linear with negative slope [$D(a)$], constant near zero [$D(b)$], and nearly constant near -5 ps nm^{-1} km^{-1} [$D(c)$]. These curves arise because of the balance between waveguide dispersion D_W curves and that of $-D_{\mathrm{mat}}$ shown in the bottom part of the figure. Note that, whereas these designs have appropriate dispersion characteristics for $N_r \geq 6$, their geometric losses impose much more stringent requirements on the number of rings, and the effective area of the fundamental mode A_{eff} is $\sim$36.5 μm^2 for $N_r = 6$. For example, for the MOF with ultraflat dispersion close to zero, $N_r \geq 18$ (1026 holes) is required for losses to be kept below 1 dB/km at $\lambda = 1.55\ \mu$m. Some laboratories have already drawn 11-ring fibers[6] (around 396 holes), there is clearly a technological interest in investigating designs that can deliver tailored dispersion characteristics with many fewer MOF rings.

To provide MOF designs that display a desirable combination of ultraflat dispersion, low-loss and quasi-single-mode operation, and a practical value of N_r, a natural strategy is to allow the hole diameter to differ from one ring to another (see Fig. 2, inset) with exterior rings that have large holes to lower the losses. We start the design process with a three-ring MOF; d_1 is arbitrarily set to $d_1 = 0.5\ \mu$m. In pursuing designs of this sort it is advantageous to employ the following scaling relation for waveguide dispersion (this is a generalization of a result given in Ref. 2):

$$D_W(\lambda, \Lambda/\Lambda_{\mathrm{ref}}, f_1, f_2, \ldots, f_n) \simeq \frac{\Lambda_{\mathrm{ref}}}{\Lambda} D_W(\lambda\Lambda_{\mathrm{ref}}/\Lambda, 1, f_1, f_2, \ldots, f_n), \quad (1)$$

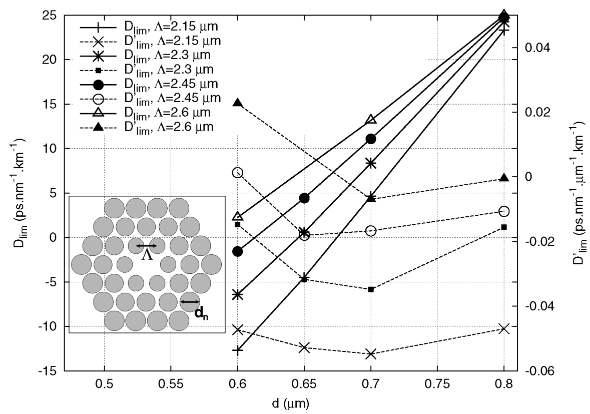

Fig. 2. Limit dispersion (solid lines, left y scale) and limit dispersion slope (dashed lines, right y scale) at $\lambda = 1.55\ \mu$m as a function of hole diameter d only, for several pitches. The chosen parameter values for Λ and d correspond to the small limit slope region. Inset, cross section of the modeled MOF with three rings of holes (holes are shown shaded), $N_r = 3$. Λ is the hole spacing and d_n is the hole diameter of the nth ring. The solid core consists of one missing hole in the center of the structure.

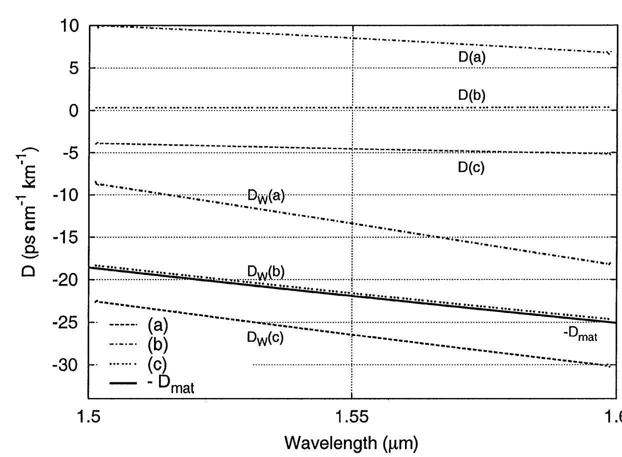

Fig. 3. Waveguide dispersion D_W, dispersion D, and sign-changed material dispersion $-D_{\mathrm{mat}}$ for three six-ring MOF structures. The line style of a MOF structure is identical for D_W and D. Λ and the diameters are given in micrometers. (a) $\Lambda = 2.3$, $d = 0.7$; (b) $\Lambda = 2.45$, $d = 0.6$; (c) $\Lambda = 2.3$, $d = 0.6$.

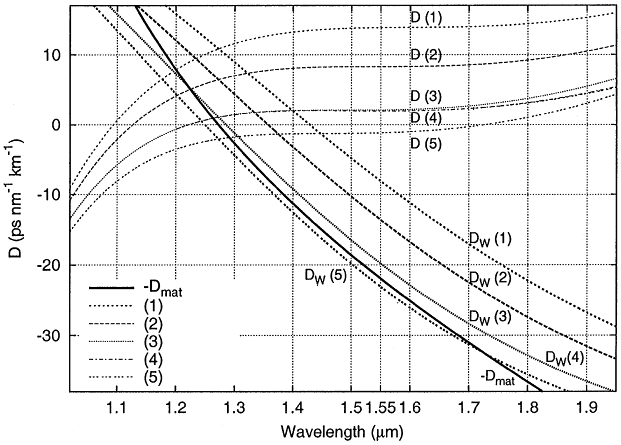

Fig. 4. Waveguide dispersion D_W, dispersion D for the MOF structures that we proposed, and sign-changed material dispersion $-D_{\mathrm{mat}}$. Unless stated, the total number of rings N_r in the MOF is three. The line style of a MOF structure is identical for D_W and D. Λ and the diameters are given in micrometers. d_n is the hole diameter of the nth ring, and $d_{n_1-n_2}$ denotes the hole diameter of the n_1th to n_2th rings. (1) $\Lambda = 1.9$, $d_1 = 0.559$, $d_2 = 0.782$, $d_3 = 0.894$; (2) $\Lambda = 1.8$, $d_1 = 0.529$, $d_2 = 0.741$, $d_3 = 0.847$; (3) $\Lambda = 1.7$, $d_1 = 0.5$, $d_2 = 0.7$, $d_3 = 0.8$; (4) $N_r = 4{-}7$, $\Lambda = 1.7$, $d_1 = 0.5$, $d_2 = 0.7$, $d_{3-7} = 0.8$; (5) $\Lambda = 1.65$, $d_1 = 0.485$, $d_2 = 0.679$, $d_3 = 0.776$.

where Λ_{ref} is the pitch of a reference lattice and f_n is the ratio d_n/Λ. Using the above scaling law and a rough optimization process on d_2, d_3, and Λ, we found an ultraflat dispersion over a long wavelength interval (approximately [1.45, 1.65] μm) for $d_2 = 0.7$ μm, $d_3 = 0.8$ μm, and $\Lambda = 1.7$ μm [$D(3)$ in Fig. 4]. It must be pointed out that the MOF design can be started from other values of d_1: For example, with $d_1 = 0.6$ μm we found $d_2 = 0.8$ μm, $d_3 = 1.0$ μm, and $\Lambda = 2.0$ μm (data not shown).

Using the scaling law [expression (1)], we can easily derive other structures that have ultraflattened chromatic dispersion but near a different value of D. Three examples of such structures, derived from the reference configuration ($d_1 = 0.5$ μm, $d_2 = 0.7$ μm, $d_3 = 0.8$ μm, $\Lambda = 1.7$ μm), are given in Fig. 4 $\{\Lambda = 1.65$ μm [$D(5)$], 1.8 μm [$D(2)$], 1.9 μm [$D(1)$]$\}$. Note that varying the pitch too far results in structures that no longer exhibit ultraflat dispersion; this is so because of the finite length of the ultraflat region in the chosen reference MOF design (data not shown).

We now control losses by adding further rings of holes with fixed diameter 0.8 μm. As can be seen from Fig. 4, adding rings 4–7 has almost no effect on the dispersion properties of the MOF [$D(4)$] but results in acceptably low values of geometric loss for technological applications: With $N_r = 6$, the losses are below 10 dB km^{-1}, and with $N_r = 7$ the losses are below 0.2 dB km^{-1}. For $N_r = 6$, the amplitude of dispersion variation is less than 3.0×10^{-2} ps nm^{-1} km^{-1} in the wavelength interval [1.5; 1.6] μm. These designs thus attain our goal of achieving ultraflat dispersion combined with low geometric loss in a MOF feasible by use of current fabrication technology. Note that one can use designs in which the outer boundary of the confining region is either hexagonal or circular. For the well-confined modes that we deal with here ($A_{\mathrm{eff}} \simeq 10.5$ μm^2 for $N_r = 6$), this difference has no practical effect on dispersion (data not shown). One interesting consequence of using three different hole diameters is that the possibility arises of having modes higher than the fundamental confined between rings of holes with different diameters. Indeed, the second mode in the seven-ring structure of Fig. 4 is confined between the first and second rings of holes and has losses approximately ten thousand times larger than that of the fundamental. This mode would not couple readily to the fundamental mode in the design, because mode energy is concentrated in different regions for the two modes and the real parts of their effective indices are quite different.

In conclusion, we have numerically demonstrated that nearly zero or nonzero ultraflattened chromatic dispersion with low loss can be achieved by use of either of two types of MOF design. The more complex design, proposed in this Letter, which has three different hole diameters, allows us to achieve low losses with many fewer air holes than with the conventional design. The design principles introduced here, together with the powerful control of dispersion given by the MOF geometry, should facilitate effective chromatic dispersion management over a wide spectral range in optical fibers.

This work benefited from travel support from the French and Australian governments.

References

1. D. Mogilevstev, T. Birks, and P. St. J. Russell, Opt. Lett. **23,** 1662 (1998).
2. A. Ferrando, E. Silvestre, J. Miret, and P. Andrés, Opt. Lett. **25,** 790 (2000).
3. A. Ferrando, E. Silvestre, P. Andrés, J. Miret, and M. Andrés, Opt. Express **9,** 687 (2001), http://www.opticsexpress.org.
4. A. Ferrando, E. Silvestre, J. Miret, P. Andrés, and M. Andrés, J. Opt. Soc. Am. A **17,** 1333 (2000).
5. B. Kuhlmey, G. Renversez, and D. Maystre, Appl. Opt. **42,** 634 (2003).
6. W. Reeves, J. Knight, and P. St. J. Russell, Opt. Express **10,** 609 (2002), http://www.optics.express.org.
7. G. P. Agrawal, *Nonlinear Fiber Optics* (Academic, San Diego, Calif., 1989).
8. T. White, B. Kuhlmey, R. McPhedran, D. Maystre, G. Renversez, C. de Sterke, and L. Botten, J. Opt. Soc. Am. B **10,** 2322 (2002).
9. M. Steel, T. White, C. de Sterke, R. McPhedran, and L. Botten, Opt. Lett. **26,** 488 (2001).
10. B. Kuhlmey, T. White, G. Renversez, D. Maystre, L. Botten, C. de Sterke, and R. McPhedran, J. Opt. Soc. Am. B **10,** 2331 (2002).
11. B. Kuhlmey, M. de Sterke, R. McPhedran, P. Robinson, G. Renversez, and D. Maystre, Opt. Express **10,** 1285 (2002), http://www.opticsexpress.org.